Cobalt complexes of bulky PNP ligand: H_2 activation and catalytic two-electron reactivity in hydrogenation of alkenes and alkynes

Sébastien Lapointe,[†a] Dilip K. Pandey,[†a] James M. Gallagher,[†] James Osborne,[†] Robert R. Fayzullin,[‡] Eugene Khaskin,[†] and Julia R. Khusnutdinova[†,*]

†Coordination Chemistry and Catalysis Unit, Okinawa Institute of Science and Technology Graduate University, 1919-1 Tancha, Onna-son, Okinawa 904-0495, Japan

‡Arbuzov Institute of Organic and Physical Chemistry, FRC Kazan Scientific Center, Russian Academy of Sciences, 8 Arbuzov Street, Kazan 420088, Russian Federation

ABSTRACT: The reactivity of cobalt pincer complexes supported by the bulky tetramethylated PNP ligands Me_4PNP^R (R = ^{i}Pr, ^{t}Bu) has been investigated. In these ligands, the undesired H-atom loss reactivity observed earlier in some classical CH_2-arm PNP cobalt complexes is blocked, allowing them to be utilized for promoting two-electron catalytic transformations at the cobalt center. Accordingly, reaction of the formally $Co^{I}Me$ complex **3** with H_2 under ambient pressure and temperature afforded the Co^{III} trihydride **4-H**, in a reaction cascade reasoned to proceed by two-electron oxidative addition and reductive eliminations. This mechanistic proposal, alongside the observance of alkene insertion and ethane production upon sequential exposure of **3** to ethylene and H_2, prompted an exploration into **3** as a catalyst for hydrogenation. Complex **4-H**, formed *in situ* from **3** under H_2, was found to be active in the catalytic hydrogenation of alkenes and alkynes. The proposed two-electron mechanism is reminiscent of the platinum group metals and demonstrates the utility of the bulky redox-innocent Me_4PNP^R ligand in the avoidance of one-electron reactivity, a concept that may show broad applicability in expanding the scope of earth-abundant first-row transition metal catalysis.

INTRODUCTION

Pincer complexes have been widely studied ever since their initial descriptions and characterization by Shaw[1] and van Koten[2-3] in the 1970s. Since then, multiple modifications at the ligand framework have been done to fine tune the electronic and steric properties to obtain specific desired reactivities, including small molecule activation and catalysis.[4-5] Many transition metal pincer complexes with platinum group metals (Ru,[6-8] Rh,[9-10] Ir,[11] Os,[12-13] Pd,[14-16] Pt[17]) have been actively studied over the last few decades due to their catalytic activity in a wide range of transformations.[18] More recently, the pincer complexes of cheap and abundant first-row transition metals have been studied extensively with the ultimate goal of their utilization for sustainable and economically viable catalytic reactions. In particular, hydrogenation of alkenes and alkynes traditionally requires precious metal catalysis. Only relatively recently, competitive base metal catalysts have been reported to be active in alkene and alkyne hydrogenation, including complexes of Fe,[19-20] Ni,[21-22] Mn,[23] and other metals.[24-25] Among these catalysts, complexes containing pincer ligands are particularly widespread, leading to active and well-defined catalysts. For example, Kirchner and co-workers recently reported Mn[26] and Fe[27] pincer catalysts for hydrogenation of alkenes and semihydrogenation of alkynes, respectively. Cobalt pincer complexes were reported active in hydrogenation of alkenes and semihydrogenation of alkynes.[28] A recent extensive review by Beller and coauthors describes the importance and activity of cobalt pincer complexes in catalysis.[29]

The basic organometallic reactivity of classical pyridine-based PNP Co complexes has also been studied by the Milstein and Chirik groups.[30-33] Milstein and co-workers reported a (PNP)CoMe complex that loses an H-atom from the CH_2 arm of the PNP ligand leading to the formation of a complex with the radical delocalized over the ligand backbone.[34] Chirik and co-workers studied in detail the reactivity of pyridine-based (PNP)Co complexes in H-atom loss, small molecule activation[30, 32, 35] and catalysis.[31, 36-38] Interestingly, the Chirik group reported that the (PNP)CoMe complex was found to activate H_2, but the catalytic activity in alkene hydrogenation was poor. The authors proposed that the lack of catalytic alkene hydrogenation was presumably due to the overstabilization of Co^{III} trihydride, which prevented H_2 reductive elimination to form the Co^{I} hydride required for subsequent alkene insertion.

The Milstein and Chirik systems suffer from possible radical formation during catalysis, that would not occur with a second- or third-row metal. One electron reactivity by first-row transition metals is a promising area of catalytic research but can be a common problem when attempting to replicate the two-electron reactivity of the more expensive second- and third-row metal catalytic systems in coupling and hydrogenation reactions. Some successful attempts in two-electron reactivity with pincer systems were shown with Fe and Co pincer complexes for the oxidative addition of H_2, HBPin, and other substrates.[30, 33, 39-40]

Our group has been interested in modifications of the classical pyridine-based PNP ligand motifs that could lead to alterations in reactivity. In particular, we developed a new bulky, electron-rich tetramethylated Me_4PNP^R (R = ^{i}Pr, ^{t}Bu) ligands, in which

ligand arm deprotonation is disabled and additional steric bulk is introduced through four Me groups on the ligand arms. We earlier reported on the stabilization of unusual Ni(I) complexes, in which the geometry around the metal atom is highly dependent on ligand sterics.[41-42] Khaskin et al. also reported that Ru complexes with Me_4PNP^R activate H_2 in an orthogonal way to classical (PNP)Ru-systems, showing a preference for cis-dihydride formation via Ru(0) intermediates, essentially introducing classical two-electron redox chemistry into a system that previously operated via only Ru(II) and metal-ligand cooperative substrate activation. [43]

The above reports suggested that Me_4PNP^R can curtail ligand-centered radical formation and that two-electron redox chemistry pathways may be more likely in the chemistry of first-row metals.

In this work, we investigated the reactivity of (Me_4PNP^R)Co complexes in small molecule activation and hydrogenation of alkenes and alkynes. Interestingly, we found that these complexes show catalytic activity in alkene and internal alkyne hydrogenation. We also observed reversible insertion of ethylene into cobalt hydride showing that reductive elimination/oxidative addition of H_2 and insertion of ethylene occur easily under mild conditions with Me_4PNP^{iPr}.

RESULTS AND DISCUSSION

Synthesis and characterization of cobalt complexes.

The Co^{II} complex **1** was prepared by reacting the previously reported tetramethylated Me_4PNP^{iPr} [41] pincer ligand with anhydrous cobalt(II) chloride precursor at room temperature overnight to afford complex **1** (Me_4PNP^{iPr})$CoCl_2$ obtained in 90% yield as a dark brownish solid. Similarly, reacting Me_4PNP^{tBu} [41] with anhydrous cobalt(II) chloride afforded (Me_4PNP^{tBu})$CoCl_2$ (**2**) as a purple solid in 92% yield (See Scheme 1). Paramagnetic complexes **1** and **2** were characterized by HRMS, UV-vis and FT-IR spectroscopy, and X-ray diffraction.

Scheme 1. Synthesis of cobalt complexes 1 and 2.

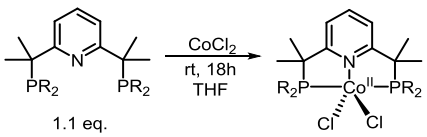

Complex **1** shows a distorted trigonal bipyramidal geometry with P1–Co1–P2, N1–Co1–Cl1, and N1–Co1–Cl2 angles of 166.704(10)°, 120.78(2)°, and 119.96(2)°. The geometry index (τ_5) of complex **1** is 0.77 (τ_5 = 1 is expected for the ideal trigonal bipyramidal geometry).[44] The Co–N distance is 2.0074(7) Å, and Co–P distances are 2.2378(2) and 2.2415(2) Å (Figure 1).

The presence of the bulkier ^{t}Bu groups on the phosphines causes a change in geometry around the metal center, pushing one chloride atom up and the other almost in the plane with the pyridine ring. Complex **2** adopts a distorted square pyramidal geometry and contains two molecules in the asymmetric unit in the crystal. Complex **2** (the first independent molecule) has P1–Co1–P2, N1–Co1–Cl1, and N1–Co1–Cl2 angles of 138.15(3)°, 163.25(7)°, and 92.64(7)°, respectively; the interatomic distances Co–N (2.342(3) Å) and Co–P (2.4610(9)-2.4691(9) Å) are consistently longer compared to complex **1**, presumably affected by the steric bulk of ^{t}Bu groups at the phosphines. The second independent molecule has similar bond distances, however it contains disordered fragments. The complex has a τ_5 value of 0.31-0.42, with a slight preference for square pyramidal over the trigonal bipyramidal structure (the ideal trigonal bipyramidal geometry is characterized with τ_5 = 0).[44] Table 1 compares the structural parameters of the two complexes.

The magnetic moment of complex **2** measured by the Evans method in CD_2Cl_2 solution at RT gives a μ_{eff} value of 4.25 μ_B, consistent with a high spin $S = 3/2$ state. Accordingly, magnetic susceptibility measurements in the solid state confirm a high spin cobalt(II) center with a χ_M·T value of 2.80 K·cm^3·mol^{-1} at 300 K, corresponding to a μ_{eff} of 4.73 μ_B (see SI for more details). Complex **1** exhibits a μ_{eff} value of 3.10 μ_B in CD_2Cl_2 solution at RT measured by the Evans method, which is intermediate between the values expected for high spin and low spin complexes, showing significant contribution of the high spin state for cobalt(II). Accordingly, the magnetic susceptibility measurements for **1** in the solid state show a χ_M·T of 2.64 K·cm^3·mol^{-1} at 300 K, corresponding to a μ_{eff} of 4.60 μ_B , however, no well-defined plateau regions were observed with χ_M·T gradualy rising from 3 to 300 K, suggesting that an incomplete spin transition occurs in this temperature range.[45-47]

Both complexes are sensitive to oxygen and decompose upon exposure to air. Exposure of **1** to O_2 affords a polymeric oxidation product **1-O₂** containing a fully oxidized phosphine ligand coordinated to a $CoCl_2$ moiety through interaction with the oxygen atom of a phosphine oxide group (see SI, Figure S56).

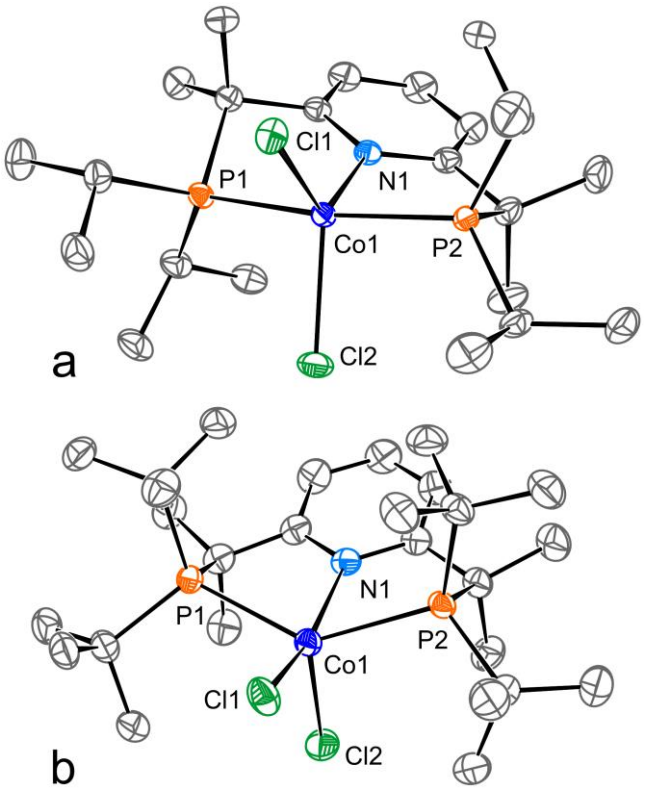

Figure 1. ORTEP of complexes 1 (a) and 2 (b) at the 70 % (1) and 50 % (2) probability level. Hydrogen atoms are omitted for clarity. In the case of 2, one of two symmetrically independent molecules is shown.

Table 1. Bond distances (Å) and angles (deg) of cobalt dichloride complexes 1 and 2 in the crystals

Complex	Co1–N1	Co1–P1	Co1–P2	Co1–Cl1	Co1–Cl2	P1–Co1–P2	N1–Co1–Cl1	N1–Co1–Cl2	Cl1–Co1–Cl2	τ_5
1	2.0074(7)	2.2378(2)	2.2415(2)	2.3423(2)	2.3159(2)	166.704(10)	120.78(2)	119.96(2)	119.255(9)	0.77
2[a]	2.342(3)	2.4691(9)	2.4610(9)	2.3056(9)	2.3017(9)	138.15(3)	163.25(7)	92.64(7)	104.11(4)	0.42
	2.343(2)	2.4702(9)	2.4921(10)	2.3326(8)	2.3034(10)	141.04(3)	159.70(8)	94.13(7)	106.17(4)	0.31

[a] The crystal structure of complex **2** contains two molecules per the asymmetric cell. Two lines represent geometrical parameters for each molecule.

Scheme 2. Synthesis of the methyl complex 3.

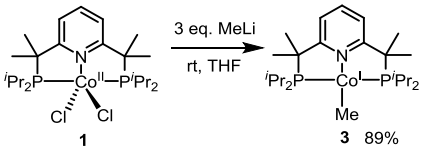

1 3 89%

Reacting complex **1** with 3 equivalents of a 3 M methyl lithium (MeLi) solution in dimethoxymethane resulted in an instantaneous color change, and produced the methyl complex **3**, (Me_4PNP^{iPr})CoMe, in 89% yield as a black powder (see Scheme 2 and Figure 2). The use of MeLi over other methylating agents, such as dimethyl zinc ($ZnMe_2$), was preferred as the latter was observed to form the cationic methyl complex with $Zn_2Cl_6^{2-}$ as a counterion. The nature of the complex [(Me_4PNP^{iPr})CoMe]$_2$[Zn_2Cl_6] was confirmed by X-ray diffraction studies without further investigations (see SI, Figure S58).

No degradation of complex **3** was observed in the solid state or solution under an inert atmosphere at room temperature for several days. Attempts to prepare a methyl complex using the bulkier Me_4PNP^{tBu} in a similar manner to the preparation of **3** proved unsuccessful, possibly due to the increased steric hindrance from the ^{t}Bu groups combined with the bulky methyl groups on the arms. Even in the presence of excess methylating agent, only chloro-complex **2** was observed. A mixture of products was observed when **2** was treated with 10 equiv of more reactive dry MeLi in diethyl ether, unlike in the previously reported procedure.[34] Attempted reactivity of **2** with NaH, $LiAlH_4$ and $NaBH_4$ also failed to form a well-defined, stable product.

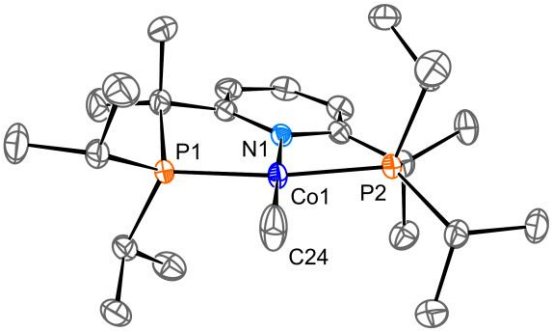

Figure 2. ORTEP of complex 3 at the 70 % probability level. Hydrogen atoms are omitted for clarity. Selected interatomic distances [Å]: Co1–P1 2.1477(3), Co1–P2 2.1437(3), Co1–N1 1.8954(8), Co1–C24 1.9949(12).

The ^{1}H NMR spectrum of the methyl complex **3** shows a methyl signal in the high field region of –1.54 ppm in toluene-d_8 as a triplet split from two P atoms with a coupling constant of 9.6 Hz (SI, Figure S3). The pyridine backbone CH proton peaks appear at 9 ppm and 5.1 ppm for the *para* and *meta* protons, respectively. The ^{13}C{^{1}H} spectrum for **3** also shows a triplet signal in the high field region for the cobalt-bound methyl group at –25.27 ppm split from two P atoms with a coupling constant of 24 Hz (Figure S4 in SI). Complex **3** shows a broad signal in ^{31}P{^{1}H} NMR at 71.65 ppm. X-ray diffraction analysis of the Co^I methyl complex **3** shows a close to ideal square planar geometry around the methyl center, with P1–Co1–P2 and N1–Co1–C24 angles of 170.935(12)° and 177.62(5)°, with a geometry index τ_4' of 0.06 (τ_4' = 0 corresponds to the ideal square planar geometry).[48-49] The Co1–C24 bond distance for the methyl group is 1.9949(12) Å, while the Co1–N1 distance is 1.8954(8) Å (Figure 2).

Reactivity of cobalt complexes with H_2 and ethylene. The Co^I methyl complex **3** readily reacts with H_2 or D_2 in solution to form the Co^{III} hydride species **4-H** or **4-D**, respectively. ^{1}H NMR analysis of **4-H** at room temperature shows a signal in the hydride region at –13.66 ppm in toluene-d_8, which splits into two signals for the axial hydrogens and the equatorial hydrogens when the temperature is lowered to –60 °C, at –9.45 ppm and –22.38 ppm, respectively. The chemical shifts are consistent with the similar (PNP^{iPr})Co^{III} trihydride previously reported by Chirik.[33] In contrast to the starting Co^I methyl complex **3**, complex **4-H** shows a downfield shifted ^{31}P{^{1}H} NMR signal at 137.52 ppm. Similarly, the reaction with D_2 gas results in the formation of the corresponding trideuteride complex **4-D** (Scheme 3), characterized by a similar ^{31}P{^{1}H} signal at 138.10 ppm.

Along with the formation of the Co^{III} hydride species **4-H**, we observe the formation of methane when **3** is reacted with H_2 gas, as a representative signal at 0.16 ppm (C_6D_6). In the case of the formation of deuteride species **4-D**, we observe a characteristic 1:1:1 signal assigned to the formation of CH_3D at 0.15 ppm as well as a small amount of methane at 0.17 ppm (see Figure S19 in SI and mechanistic discussion below).

The T_1 relaxation time measurements for the Co-H signals are consistent with its assignment as the classical trihydride complex with a T_1 value (minimal, 400 MHz) of 74 ms and 64 ms at -60 °C for axial and equatorial Co-H signals respectively (See Table S1 in the SI). These values are typical for hydrides [50-54] and are similar to the values reported for Co trihydride complexes with pyridine-based[33] and aliphatic PNP ligands.[55] The axial Co-H peak appears as a triplet of doublets with splitting from two P-atoms (J_{HP} = 42 Hz) and the equatorial Co-H (J_{HH} = 16 Hz) (Figure S17), with an H-H coupling constant similar to the values reported for PNP Co trihydride complexes.[55] The equatorial Co-H signal appears as a broadened triplet of triplets

with similar coupling constants (J_{HP} ~ 49 Hz and J_{HH} ~16 Hz). Overall, the T_1 measurements and splitting patterns are consistent with the assignment of this complex as a classical trihydride rather than a Co^I-coordinated H_2 complex.

Scheme 3. Reactivity of complex 3 with H_2 and D_2.

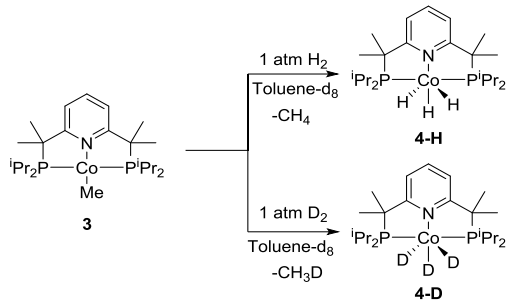

X-ray diffraction studies of **4-H** and **4-D** show that the geometry around the metal center is octahedral with no exceptional distances or angles (Figure 3). H-atoms at the octahedral Co-center were found directly from difference Fourier maps and refined isotropically. The Co-H distances are 1.462(15), 1.475(16), and 1.458(15) Å, while H...H distances are higher than 1.9 Å, also consistent with the assignment of **4-H** as a classical trihydride complex.

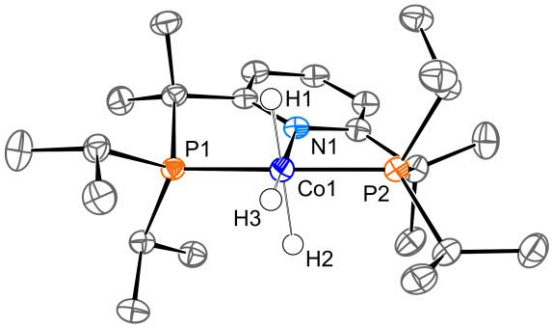

Figure 3. ORTEP of complex 4-H at the 70 % probability level for nonhydrogen atoms. Hydrogen atoms are omitted for clarity, except for those at the metal center. Selected interatomic distances [Å]: Co1–P1 2.1108(4), Co1–P2 2.1121(4), Co1–N1 1.9716(11), Co1–H1 1.462(15), Co1–H2 1.475(16), Co1–H3 1.458(15).

Scheme 4. Reactivity of 4-H with ethylene.

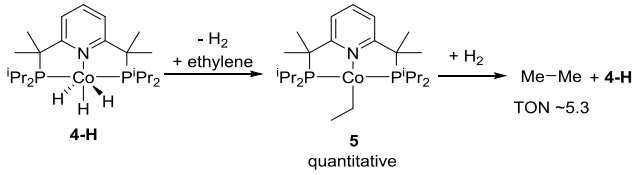

Reacting **4-H** in the presence of 1 atmosphere of ethylene leads to a rapid color change of the red solution to dark brown, and the quantitative formation of an ethyl cobalt complex, (Me_4PNP^{iPr})Co^IEt, **5** (Scheme 4). This reaction is accompanied by the formation of a small amount of ethane (24% yield based on Co), suggesting concomitant hydrogenation of the ethylene by **4-H** and residual H_2. The formation of **5** is confirmed by ^1H NMR with the ethyl α-carbon signal at –0.34 ppm and the β-carbon at 0.67 ppm. $^{13}C\{^1H\}$ NMR of **5** is characterized by the peak of the α-carbon at –15.64 ppm and the peak of the β-carbon at 18.28 ppm. Complex **5** shows a broad signal in the $^{31}P\{^1H\}$ NMR at 74.21 ppm, similar to the cobalt-methyl species **3** (71.65 ppm). Despite multiple crystallization attempts, we were not able to obtain a crystal of the ethyl complex suitable for X-ray diffraction studies, most likely due to the formation of ethylene through β-hydride elimination. The solution shows decomposition via the formation of solids upon long-standing times even under an ethylene atmosphere.

Evacuation of the atmosphere and addition of H_2 (1 bar) reformed **4-H** as a dark red solution along with free ethane, which was formed with a TON 5.3 due to the hydrogenation of dissolved ethylene. NMR analysis showed that the **4-H/5** cycle could be repeated multiple times (with the caveat the complexes are only temporarily stable in solution) upon repeated evacuation/refilling with ethylene / H_2 (see Figures S26 and S27 in SI). These facile and reversible transformations suggested that complex **4-H** may be catalytically active in alkene hydrogenation.

Hydrogenation of alkynes and alkenes catalyzed by 3 as a pre-catalyst

The aforementioned interconversion of **4-H** and **5** led us to use complex **3** as a pre-catalyst (forming **4-H** *in-situ*) for the hydrogenation of alkenes and alkynes. We first tested the catalytic activity of **3** in hydrogenation using diphenylacetylene as a model substrate. Since using catalyst loadings below 1 mol% resulted in a slow reaction, we performed the catalytic tests at higher catalyst loadings and 5 bar of H_2 at 100 °C. After one hour in the presence of 2 mol% **3**, we initially observed the formation of *cis*-stilbene and *trans*-stilbene in 16% and 3% yields, respectively (Table 2, entry 1). After 24 h, *cis*-stilbene was observed a major product formed in 73% yield, while *trans*-stilbene is observed in only 16%, and only a trace amount of fully hydrogenated product, bibenzyl, was present in 2% (Table 2, entry 2). Further increasing the reaction time to 48 h leads to a higher fraction of *trans*-stilbene (30% vs. 56% of *cis*-stilbene) along with a higher amount of bibenzyl (7%) showing that *cis-trans* isomerization occurs under the reaction conditions (Table 2, entry 3).

When the catalyst loading was increased to 5 mol%, an overall faster reaction led to the exclusive formation of *trans*-stilbene after 24 h, which is then slowly converted to bibenzyl at 100 °C (Table 2, entries 5 and 6). *cis*-Stilbene forms at the initial stages of the reaction, and then slowly disappears upon further heating (Figure S38).

Table 2. Partial and full hydrogenation of diphenylacetylene catalyzed by 3 under 5 bar of H_2.

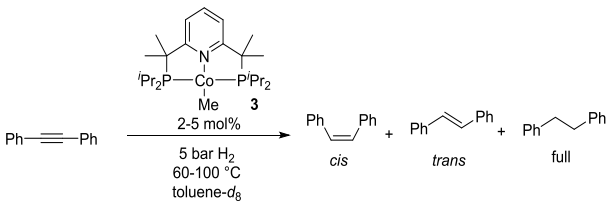

Entry	Catalyst loading (mol%)	T (°C)	Time	NMR yield[a] (%) *cis*:*trans*:full
1	2	100	1 h	16:3:0
2	2	100	24 h	73:16:2
3	2	100	48 h	56:30:7
4	5	100	1 h	57:33:4

5	5	100	24 h	0:86:15
6	5	100	48 h	0:70:26
7	5	80	1 h	34:4:0
8	5	80	24 h	17:76:7
9	5	80	48 h	2:90:9
10	5	80	72 h	0:94:9
11	5	60	1 h	30:3:0
12	5	60	24 h	80:13:2
13	5	60	48 h	66:26:4
14	5	60	72 h	57:35:5
15	None	100	72 h	N.R.[c]

[a] Yields were determined by NMR using mesitylene as an internal standard. Typical conditions: Substrate (0.042 mmol) and mesitylene standard solution in toluene-d_8 containing pre-catalyst **3** were placed in a pressure NMR tube, pressurized with 5 bar of H_2, and heated at a constant temperature. Periodically the reaction mixture was cooled down to RT and analyzed by NMR.

When the reaction was performed at lower temperatures (60 or 80 °C) while maintaining the 5 mol% catalyst loading, higher selectivity could be obtained for the formation of *cis*-stilbene at intermediate reaction times (Figures 4 and S40). For example, the reaction profile of the formation of stilbenes and bibenzyl was monitored at 80 °C, showing that the maximum yield of *cis*-stilbene (87%) could be obtained after a 4 h reaction time. (Figure 4).

The hydrogenation of the aliphatic internal alkyne, 4-octyne, at 100 °C and 5 bar H_2 catalyzed by 5 mol% of **3** gave only the *trans*-alkene product even at incomplete conversion and intermediate reaction times (see SI, Table S1), with full conversion to *trans*-4-octene observed after 24 h (Table 3, entry 1).

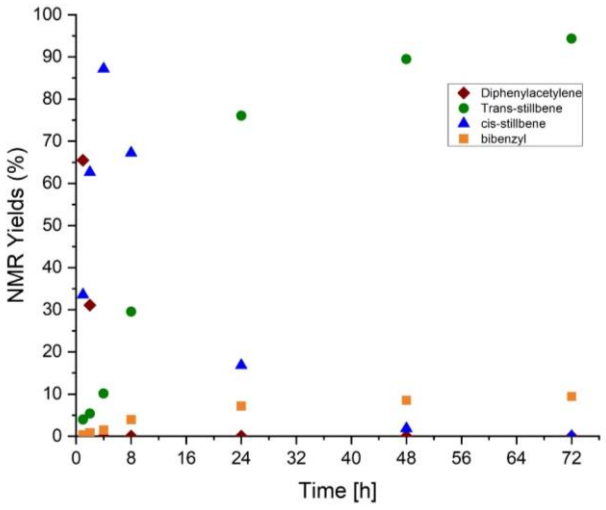

Figure 4. Yields of reaction products and starting reactants for the hydrogenation of diphenylacetylene using 5 mol% of pre-catalyst 3 at 80 °C over 72 h. Conditions are shown in the caption of Table 2.

Table 3. Hydrogenation of internal alkynes, terminal and internal alkenes catalyzed by 3 under 5 bar of H_2.

Entry	Substrate	Product	Conditions	Yield (%)[a]
1	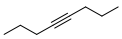		toluene-d_8, 100 °C: 8 h 24h	43 >99
2	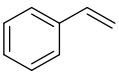	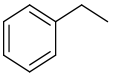	toluene-d_8, 100 °C, 24 h	99
3	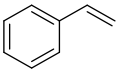	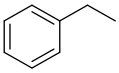	THF-d_8, RT, 16 h	96
4			toluene-d_8, 100 °C, 24 h	>99
5	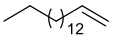	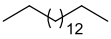	THF-d_8, RT, 16 h	>99
6			toluene-d_8, 100 °C, 24 h	97
7		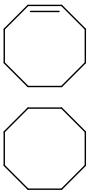	toluene-d_8, 100 °C, 24 h	23 77

[a]Yields were determined by NMR using mesitylene as an internal standard. Experiments without catalysts under the same reaction conditions showed no catalytic activity. Reaction conditions: 5 mol% of complex **3** (0.0021 mmol), substrate (0.042 mmol), mesitylene (0.021 mmol), solvent (THF-d_8 or toluene-d_8, 0.6 mL), 5 bar of H_2 in a high-pressure NMR tube.

We also tested **3** in the hydrogenation of terminal and internal alkenes. Quantitative hydrogenation of styrene and 1-hexene was observed upon heating alkene with 5 mol% of **3** in toluene-d_8 at 100 °C for 24 h (Table 3, entry 2). Gratifyingly, hydrogenation of styrene and most unactivated aliphatic alkenes proceeds at much milder conditions: at RT under 5 bar of H_2 and 5 mol% of **3**, giving the corresponding hydrogenated products in high yields (Table 3, entries 3 and 5).

By contrast, internal alkenes (as well as internal alkynes) are unreactive at RT, and their hydrogenation required heating at 100 °C to obtain good conversion. *cis*-Cyclooctene could be hydrogenated to cyclooctane in almost quantitative yield after 24 h, while 1,5-cyclooctadiene gave a mixture of cyclooctane and *cis*-cyclooctene in 77% and 23% yields, respectively, after heating at 100 °C for 24 h in toluene-d_8 (Table 3, entries 6 and 7).

Based on the observed reactivity with ethylene described above, we propose that catalytic hydrogenation of alkenes proceeds through a sequence of oxidative addition (OA)/reductive elimination (RE) steps at the Co^{III}/Co^{I} intermediates (Scheme 5). First, the formation of the active hydride catalyst proceeds through initial oxidative addition of H_2 to **3** followed by reductive elimination of methane to form a transient Co^{I} hydride species, which immediately undergoes oxidative addition under H_2 pressure to form the more stable Co^{III} trihydride **4-H**. Reversible H_2 elimination from **4-H** may regenerate the catalytically active Co^{I} hydride species, which undergoes alkene insertion in

the presence of excess substrate. This is followed by another step of H_2 oxidative addition and C–H reductive elimination to produce the product and regenerate the Co^I hydride intermediate.

A similar mechanism is also expected for internal alkyne hydrogenation leading to the initial formation of a *cis*-isomer which then undergoes *cis*/*trans* isomerization under thermal conditions. This is consistent with the initial fast appearance of a *cis*-stilbene during hydrogenation of 1,2-diphenylacetylene, which then slowly undergoes conversion to *trans*-stilbene. The stilbenes can also be converted to the fully hydrogenation bibenzyl product (Figure 4 and Figures S39-S42 in the Supporting Information). Consistent with the proposed mechanism, we observed characteristic temperature-dependent color changes during a typical hydrogenation reaction. In the presence of **3**, 5 bar of H_2, a substrate, the color of the solution changes from an initial orange color characteristic of **4-H** to a dark brown color upon heating, which is indicative of the formation of a cobalt(I) species in solution (for reference, the color of both **3** and the ethyl complex **5** is brown in solution). The color reverts to orange when the solution is cooled down to RT and persists until the solution is heated again, consistent with Co^{III}/Co^I interconversion.

Scheme 5. Proposed mechanism for the active catalyst formation (a) and catalytic hydrogenation of alkenes (b).

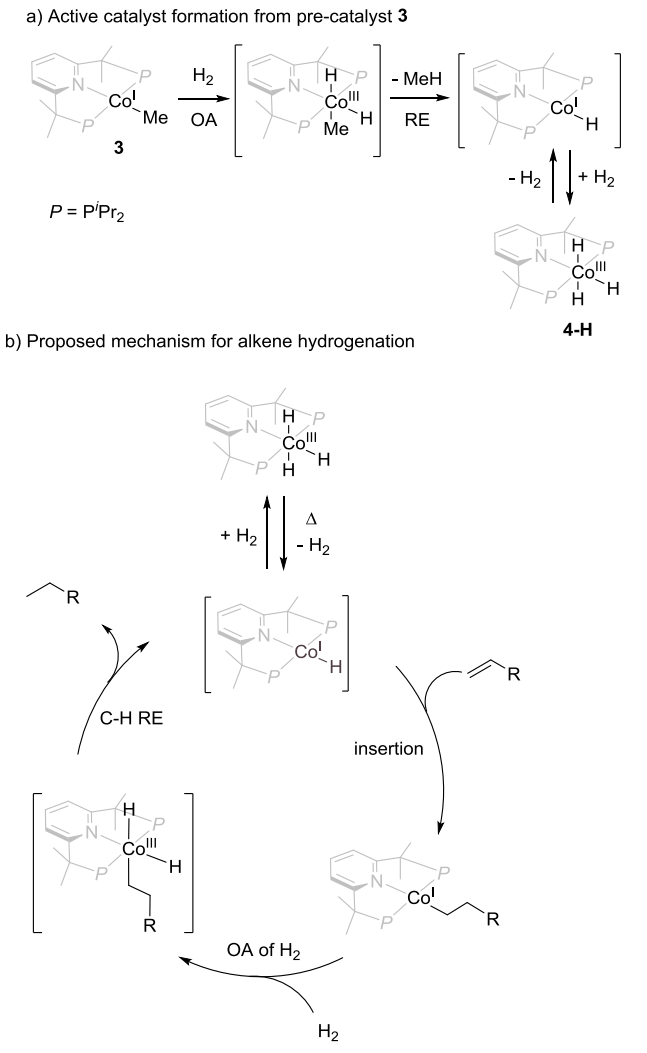

SUMMARY AND CONCLUSION

We have prepared a new family of cobalt pincer complexes containing the bulky tetramethylated Me_4PNP^R (R = ^{i}Pr, ^{t}Bu) pincer ligands, and we explored the reactivity toward MeLi and H_2, as well as the catalytic hydrogenation of alkynes and alkenes with Me_4PNP^{iPr} supported complex **4-H**. Reacting complex **1** with methyl lithium affords the methyl-bound complex **3**, which can easily undergo oxidative addition in the presence of H_2 or D_2 to form the octahedral cobalt(III) species **4-H** or **4-D**. Addition of ethylene to a solution of **4-H** produces the ethane-bound cobalt(I) species **5** which has been characterized by NMR, but slowly decomposes even under an ethylene atmosphere. The formation of **5** is reversible, and it reforms **4-H** under H_2, leading us to explore the catalytic activity of **4-H** in hydrogenation of alkenes and alkynes. Complex **3** was used as a pre-catalyst for the reaction. We were able to hydrogenate unactivated hydrocarbon internal and terminal alkynes and alkenes successfully. The best results were obtained at 100 °C under 5 bar H_2 and 5 mol% catalyst loading.

The addition of methyl groups on the pincer's arms prevents the undesirable formation of radical species in **3**, in contrast to the classical PNP cobalt methyl complex previously shown by Milstein.[34] Preventing side-reaction through modification of the ligand framework could be beneficial in cobalt-catalyzed reactions. This forces the first-row cobalt into traditional two-electron oxidative addition / reductive elimination reactivity that is typical of more expensive second and third metals that are often used in various catalytic processes, including selective hydrogenation. In the future, we envision that this type of 'tamed' cobalt complex could be applied to other coupling reactions such as borylation of alkynes/alkenes, or alkyl and aryl halides coupling.

EXPERIMENTAL SECTION

All operations were performed using standard Schlenk or glovebox techniques under a N_2 atmosphere unless indicated otherwise. Unless otherwise indicated, all solvents and reagents were used as received. Non-deuterated solvents were taken from a solvent purification system (MBRAUN SPS). Acetone-d_6 was vacuum distilled over dried magnesium sulfate at low temperature. All other deuterated solvents were added to activated 3 Å molecular sieves, except for toluene-d_8, which was dried over dry CaH_2 and filtered prior to being added to 3 Å molecular sieves. Methyl lithium 3 M in diethoxymethane was purchased from Sigma-Aldrich. Cobalt(II) chloride (anhydrous) was purchased from Merck Ltd. The ligands were prepared according to previously published procedures.[41]

NMR spectra were recorded using JEOL ECZR-400 MHz or ECZR-600 MHz spectrometers. Chemical shifts are reported in ppm (δ) and referenced internally to the residual solvent signals (^{1}H and ^{13}C: 7.26 and 77.16 ppm for $CDCl_3$; 2.05 and 29.84 ppm for acetone-d_6; 2.08 and 128.87 ppm for toluene-d_8). The signal abbreviations are as follows: d – doublet, t – triplet, v – virtual, q – quartet, br - broad, m – multiplet. The proton relaxation time T_1 measurements at variable temperature were performed in toluene-d_8 on a 399.78 MHz JEOL spectrometer. Fourier transform infrared (FT-IR) spectra were recorded on Cary 630 or Bruker Alpha II spectrometers with an attenuated-total-reflectance (ATR) module. Abbreviations are as follows: w – weak, m – medium, s – strong. UV-vis spectra were recorded on a Cary 60 UV-vis spectrophotometer. X-ray diffraction experiments were described in SI. The magnetic properties were measured using a 9T physical properties measurement system PPMS Dynacool from Quantum Design, equipped with the vibrating sample magnetometer (VSM)

option, in a 3–300 K temperature range under a magnetic field of 10 000 Oe. For these measurements, samples were ground into powder and placed in plastic capsules. The Evans method measurements were performed in the coaxial NMR tube at 298 K; diamagnetic correction was applied.[56-57]

(Me$_4$PNP^{iPr})CoCl$_2$, 1. To a solution of freshly prepared **Me$_4$PNP^{iPr}** ligand (50 mg, 0.126 mmol) in THF (10 mL) was added anhydrous cobalt(II) chloride (15 mg, 0.115 mmol). The reaction was stirred at room temperature overnight. The solution was evaporated under reduced pressure and the solid was washed with pentane and diethyl ether and dried again under vacuum to afford a dark-colored solid (54.4 mg, 0.103 mmol, 90%). Single crystals suitable for X-ray diffraction studies were grown from layering of pentanes on a concentrated dichloromethane solution of **1**. The complex is paramagnetic, and only broad signals are observed in ^{1}H NMR. ^{1}H NMR (400 MHz, acetone-d_6): δ –6.56 (br s), 3.06 (br s), 10.29 (br s), 24.99 (br s). ATR-IR (cm^{-1}): 2976 (w), 2959 (w), 2932 (w), 2873 (w), 1591 (w), 1567 (w), 1462 (m), 1443 (m), 1380 (w), 1243 (m), 1087 (w), 931 (w), 880 (w), 829 (w), 669 (s), 614 (m), 474 (w). UV-vis (THF, [1·10^{-4} M]), λ_{max}, nm (ε, L mol^{-1} cm^{-1}): 267 (7213), 355 (2737), 399 (1365, sh) 528 (1180, br). ESI-HRMS (*m/z*): calculated for [C$_{23}$H$_{43}$P$_2$CoNCl]$^+$: 489.1886 (loss of one Cl during ionization); found 489.1879. Anal. Calcd for C$_{23}$H$_{43}$Cl$_2$CoNP$_2$: C, 52.58; H, 8.25; N, 2.67. Found: C, 52.88; H, 8.06; N, 2.85.

(Me$_4$PNP^{tBu})CoCl$_2$, 2. To a solution of freshly prepared **Me$_4$PNP^{tBu}** ligand (54 mg, 0.119 mmol) in THF (10 mL) was added anhydrous cobalt(II) chloride (14 mg, 0.108 mmol). The reaction was stirred at room temperature overnight. The solution was evaporated under reduced pressure and the solid was washed with pentane and diethyl ether and dried again under vacuum to afford a purple solid (58 mg, 0.099 mmol, 92%). Purple crystals suitable for X-ray diffraction studies were grown from a concentrated acetone solution of **2** at –30 °C under N$_2$. The complex is paramagnetic, and only broad signals are observed in ^{1}H NMR. ^{1}H NMR (600 MHz, acetone-d_6): δ –0.61 (br s), 20.05 (br s), 23.17 (br s), 37.05 (br s), 58.65 (br s). ATR-IR (cm^{-1}): 3005 (w), 2969 (w), 2895 (w), 2868 (w), 1578 (w), 1573 (w), 1470 (m), 1435 (s) 1392 (w), 1369 (w), 1177 (w), 1106 (w), 990 (w), 896 (w), 817 (m) 763 (w), 729 (w), 486 (w). UV-vis (THF, [1·10^{-4} M]), λ_{max}, nm (ε, L mol^{-1} cm^{-1}): 271 (7490), 323 (2382), 366 (852, sh), 574 (340), 742 (181). ESI-HRMS (*m/z*): calculated for [C$_{27}$H$_{51}$P$_2$CoNCl]$^+$: 545.2512 (loss of one Cl during ionization); found 545.2504. Anal. Calcd for C$_{27}$H$_{51}$Cl$_2$CoNP$_2$: C, 55.77; H, 8.84; N, 2.41. Found: C, 55.70; H, 8.56; N, 2.90.

(Me$_4$PNP^{iPr})CoMe, 3. To a solution of **1** (100 mg, 0.190 mmol) in THF (10 mL) was added a solution of MeLi (3 M solution in dimethoxymethane, 190 µL, 0.190 mmol, 3.00 eq.), which turned dark brown instantly after addition. The solution was then evaporated under reduced pressure, and pentane was added. The solution was filtered through a short celite pad and evaporated under reduced pressure to afford a dark brown solid (79 mg, 0.17 mmol, 89%). Dark brown crystals suitable for X-ray diffraction were grown from a THF solution of **3** at –30 °C under N$_2$. ^{1}H NMR (500 MHz, toluene-d_8, 23 °C): δ -1.54 (t, J_{HP} = 9.6 Hz, 3H, Co-C***H*****$_3$**), 1.35-1.39 (m (overlap), 12H + 12H, P-C(C***H*****$_3$**)$_2$C$_{py}$ + PCH-C***H*****$_3$**), 1.42-1.46 (m, 12H, PCH-C***H*****$_3$**), 2.62-2.72 (m, 4H, PC***H***-CH$_3$), 5.13 (d, J_{HH} = 7.13 Hz, 2H, C$_{py}$-***H*****$_{meta}$**), 8.93 (tt, J_{HH} = 7.5 Hz, J_{HP} = 3.7 Hz, 1H, C$_{py}$-***H*****$_{para}$**). ^{13}C{^{1}H} NMR (126 MHz, toluene-d$_8$, 23 °C): δ -25.27 (t, J_{PC} = 24.1 Hz, Co-***C***H$_3$), 18.80 (PCH-***C***H$_3$), 19.97 (vt, J_{PC} = 2.6 Hz, PCH-***C***H$_3$, *overlaps with toluene-d_8, visible by DEPT-135 NMR), 22.30 (vt, J_{PC} = 6.0 Hz, P***C***H-CH$_3$), 23.99 (P-C(***C***H$_3$)$_2$C$_{py}$), 50.18 (vt, J_{PC} = 5.5 Hz, P-***C***(CH$_3$)$_2$C$_{py}$), 108.70 (vt, J_{PC} = 2.7 Hz, ***C*****$_{py,para}$**), 121.46 (vt, J_{PC} = 7.0 Hz, ***C*****$_{py,meta}$**), 165.08 (vt, J_{PC} = 7.0 Hz, ***C*****$_{py,ortho}$**). ^{31}P{^{1}H} NMR (202 MHz, toluene-d_8, 23 °C): δ 71.65 (br, s). ATR-IR (cm^{-1}): 655.08 (m), 715.65 (m), 759.45 (m), 818.15 (w), 882.45 (m), 929.97 (m), 982.15 (m), 1021.29 (m), 1083.72 (m), 1137.77 (m), 1153.61 (m), 1232.81 (s), 1292.45 (w), 1344.63 (s), 1379.11 (m), 1452.73 (m), 1562.68 (m), 1824.53 (w), 2111.53 (w), 2319.33 (w), 2789.91 (w), 2862.59 (m), 2948.32 (m). UV-vis (THF, [1·10^{-4} M]), λ_{max}, nm (ε, L mol^{-1} cm^{-1}): 262 (14937, sh), 354 (3924), 433 (6765), 517 (4967), 604 (2634), 814 (8698, br).

(Me$_4$PNP^{iPr})CoH$_3$, 4-H. To a Young tube was added a solution of **3** (10 mg, 0.02 mmol) in toluene-d_8 (1 mL) under an N$_2$ atmosphere. The Young tube was then cooled to –78 °C and evacuated for a few seconds. Then, 1 bar of H$_2$ was added in the Young tube and color change to orange is observed instantly upon mixing of the solution and the H$_2$ atmosphere. Orange crystals suitable for X-ray diffraction studies were grown in the tube under H$_2$ atmosphere overnight. This complex was prepared *in situ*, as it partially decomposed *in vacuo* or when left in the solution under an inert atmosphere in the absence of H$_2$ for over a few hours to form the free ligand. Thus, it was not possible to obtain an isolated yield, but we observed full conversion of **3** to **4-H** by NMR. ^{1}H NMR (600 MHz, toluene-d_8, 23°C): δ –13.66 (br s, Co-(***H***)$_3$), 0.16 (free methane), 1.13-1.24 (br m, 12H, PCH-C***H*****$_3$**), 1.24-1.28 (m, 12H, PCH-C***H*****$_3$**), 1.31-1.34 (m, 12H, PCH-C***H*****$_3$**), 1.54-1.56 (m, 12H, P-C(C***H*****$_3$**)$_2$C$_{py}$), 2.20-2.26 (m, 4H, PC***H***-CH$_3$), 6.32 (d, J_{HH} = 7.8 Hz, 2H, C$_{py}$-***H*****$_{meta}$**), 6.82 (t, J_{HH} = 7.9 Hz, 1H, C$_{py}$-***H*****$_{para}$**). ^{1}H NMR (600 MHz, Toluene-d$_8$, -60 °C): δ –22.38 (br s, 1H, Co-***H*****$_{eq}$**), –9.45 (br t, J_{HP} = 40.9 Hz, Co-***H*****$_{ax}$**), 0.25 (free methane), 0.77-0.99 (br m, 6H, PCH-(C***H*****$_3$**)$_2$, 1.15-1.44 (overlap br m, 12H + 6H, (PCH-(C***H*****$_3$**)$_2$)$_2$ + PCH-(C***H*****$_3$**)$_2$), 1.50-1.77 (br m, 12H, P-C(C***H*****$_3$**)$_2$C$_{py}$), 1.87-2.00 (br m, 2H, (PC***H***-CH$_3$)$_2$), 2.16-2.37 (br m, 2H, (PC***H***-CH$_3$)$_2$), 6.21 (d, J_{HH} = 8.0 Hz, 2H, C$_{py}$-***H*****$_{meta}$**), 6.76 (t, J_{HH} = 8.0 Hz, C$_{py}$-***H*****$_{para}$**). ^{13}C{^{1}H} NMR (151 MHz, C$_6$D$_6$, 23°C): δ 18.90 (PCH-***C***H$_3$), 20.76 (PCH-***C***H$_3$), 24.73 (P***C***H-CH$_3$), 26.62 (P-C(***C***H$_3$)$_2$C$_{py}$), 49.92 (vt, J_{PC} = 6.3 Hz, P-***C***(CH$_3$)C$_{py}$), 115.97 (vt, J_{PC} = 4.5 Hz, ***C*****$_{py,meta}$**), 132.88 (***C*****$_{py,para}$**), 172.38 (vt, J_{PC} = 8.0 Hz, ***C*****$_{py,ortho}$**). ^{31}P{^{1}H} NMR (243 MHz, C$_6$D$_6$, 23°C): δ 137.52 (br). ^{31}P{^{1}H} NMR (243 MHz, Toluene-d$_8$, -60°C): δ 136.52 (br). ATR-IR (cm^{-1}): 656.94 (s), 703.53 (m), 740.81 (s), 785.54 (m), 806.97 (m), 823.74 (m), 881.52 (m), 925.31 (m), 943.95 (m), 1008.24 (m), 1036.20 (m),1081.86 (m), 1110.75 (w), 1154.54 (w), 1180.63 (w), 1231.89 (m), 1252.39 (w), 1291.52 (w), 1352.09 (m), 1378.18 (m), 1454.59 (m), 1554.30 (m), 1585.05 (w), 1683.82 (s), 1753.71 (w), 1831.99 (w), 1913.06 (m), 2299.77 (w), 2323.06 (w), 2861.66 (m), 2904.53 (m), 2945.53 (m), 2965.10 (m). UV-vis (THF, [1·10^{-4} M]), λ_{max}, nm (ε, L mol^{-1} cm^{-1}): 256 (10309), 314 (2844), 386 (2111), 459 (3857), 578 (1544), 823 (2853, br). ESR-HRMS analysis was not possible due to the instability under air. Formation of phosphine oxides were the only products observed by ESI-HRMS.

(Me$_4$PNP^{iPr})CoD$_3$, 4-D. To a Young tube was added a solution of **3** (10 mg, 0.02 mmol) in toluene-d_8 (1 mL) under N$_2$ atmosphere. The Young tube is then cooled to –78 °C and evacuated for a few seconds. Then, 1 bar of D$_2$ was introduced and color changed to orange was observed instantly upon mixing. Orange crystals suitable for X-ray diffraction studies were grown in the Young tube under a D$_2$ atmosphere and were tested to have the same unit cell parameters as **4-H**, confirming that it adopts the same structure. This complex was prepared *in situ*, as it partially decomposed *in vacuo* or when left in the solution under an inert in the absence of H$_2$ for over a few hours to form the free ligand. Thus, we were not able to obtain an isolated yield, but we observed a full conversion of **3** to **4-D** by NMR. ^{1}H NMR (400 MHz, toluene-d_8, 23°C): δ 1.16-1.21 (m, 12H, PCH-C***H*****$_3$**), 1.26-1.31 (m, 12H, PCH-C***H*****$_3$**), 1.52-1.53 (m, 12H, P-C(C***H*****$_3$**)$_2$C$_{py}$), 2.13-2.22 (m, 4H, PC***H***-CH$_3$), 6.29 (d, J_{HH} = 7.8 Hz, 2H, C$_{py}$-***H*****$_{meta}$**), 6.85 (t, J_{HH} = 7.9 Hz, 1H, C$_{py}$-***H*****$_{para}$**). ^{31}P{^{1}H} NMR (243 MHz, toluene-d_8, 23°C) δ 138.10 (br).

(Me$_4$PNP^{iPr})CoEt, 5. A Young tube containing the *in situ* prepared **4-H** (5 mg, 0.01 mmol) in toluene-d_8 (1 mL) was cooled

to –78 °C, the atmosphere evacuated and 1 bar of ethylene was added to the solution when it reached room temperature. A color change to dark brown was observed after a few seconds. Complex **4-H** was fully converted to **5** and ethane under these conditions. Upon prolonged storage in solution at RT, the complex decomposes partially to the free ligand. Isolated yield could not be reported due to the lability of the cobalt-ethyl bond. ^{1}H NMR (400 MHz, toluene-d_8, 23 °C): δ –0.41 to –0.30 (m, 2H, Co-C***H***$_2$CH$_3$), 0.67 (t, J_{HH} = 7.7 Hz, 3H, Co-CH$_2$C***H***$_3$), 1.33-1.38 (m, 12H, PCH-C***H***$_3$), 1.40-1.42 (m, 12H, P-C(C***H***$_3$)$_2$C$_{py}$), 1.45-1.50 (m, 12H, PCH-C***H***$_3$), 2.65-2.73 (m, 4H, PC***H***-CH$_3$), 5.22 (d, J_{HH} = 7.7 Hz, 2H, C$_{py}$-***H$_{meta}$***), 8.79 (tt, J_{HH} = 7.1 Hz, J_{HP} = 3.2 Hz, 1H, C$_{py}$-***H$_{para}$***). ^{13}C{^{1}H} NMR (101 MHz, toluene-d_8, 23°C): δ -15.64 (br, Co-***C***H$_2$CH$_3$), 18.28 (Co-CH$_2$***C***H$_3$), 19.56 (PCH-***C***H$_3$), 20.32 (overlap with toluene-d$_8$, PCH-***C***H$_3$), 22.38 (vt, J_{PC} = 5.8 Hz, P***C***H-CH$_3$), 23.87 (P-C(***C***H$_3$)$_2$C$_{py}$), 49.64 (vt, J_{PC} = 5.9 Hz, P-***C***(CH$_3$)$_2$C$_{py}$), 109.38 (***C$_{py,para}$***), 121.57 (vt, J_{PC} = 6.2 Hz, ***C$_{py,meta}$***), 164.78 (vt, J_{PC} = 6.5 Hz, ***C$_{py,ortho}$***)

ASSOCIATED CONTENT

Supporting Information

The Supporting Information is available free of charge on the ACS Publications website at DOI:

Experimental details and characterization data (PDF)

Accession codes

CCDC 2103902-2103907 contains the supplementary crystallographic data for this paper. These data can be obtained free of charge via https://www.ccdc.cam.ac.uk/structures/.

AUTHOR INFORMATION

[a]These authors contributed equally.

Corresponding Author

*E-mail for J.R.K.: juliak@oist.jp

ORCID:

Sebastien Lapointe: 0000-0003-3190-3803

Dilip Pandey: 0000-0002-0025-2502

James Gallagher: 0000-0003-1001-0117

James Osborne: 0000-0003-0903-2546

Eugene Khaskin: 0000-0003-1790-704X

Robert R. Fayzullin: 0000-0002-3740-9833

Julia R. Khusnutdinova: 0000-0002-5911-4382

Notes

The authors declare no competing financial interests.

ACKNOWLEDGMENT

We thank Instrumental Analysis section (especially Dr. Michael Roy) and Engineering Section for technical support. We also thank Shubham Deolka for help with VT NMR. The authors acknowledge the Okinawa Institute of Science and Technology Graduate University for start-up funding. R. R. F. performed crystal structure determination within the government statements for Kazan Scientific Center of RAS.

REFERENCES

1. Moulton, C. J.; Shaw, B. L. Transition metal–carbon bonds. Part XLII. Complexes of nickel, palladium, platinum, rhodium and iridium with the tridentate ligand 2,6-bis[(di-*t*-butylphosphino)methyl]phenyl. *J. Chem. Soc., Dalton Trans.* **1976**, 1020-1024.
2. van Koten, G.; Timmer, K.; Noltes, J. G.; Spek, A. L. A novel type of Pt-C interaction and a model for the final stage in reductive elimination processes involving C-C coupling at Pt; synthesis and molecular geometry of [1,N,N'-ε-2,6-bis{(dimethylamino)methyl}-toluene]iodoplatinum(II) tetrafluoroborate. *J. Chem. Soc., Chem. Commun.* **1978**, 250-252.
3. van Koten, G.; Jastrzebski, J. T. B. H.; Noltes, J. G.; Spek, A. L.; Schoone, J. C. Triorganotin cations stabilized by intramolecular Sn-N coordination; synthesis and characterization of {C,N,N′ -2,6-bis[(dimethylamino)methyl]phenyl}diorganotin bromides. *J. Organomet. Chem.* **1978,** *148*, 233-245.
4. Peris, E.; Crabtree, R. H. Key factors in pincer ligand design. *Chem. Soc. Rev.* **2018,** *47*, 1959-1968.
5. van Koten, G.; Milstein, D. (Eds) *Organometallic pincer chemistry*. 1st ed.; Springer: Berlin; New York, 2013; p 356.
6. Gunanathan, C.; Milstein, D. Bond Activation and Catalysis by Ruthenium Pincer Complexes. *Chem. Rev.* **2014,** *114*, 12024-12087.
7. Gnanaprakasam, B.; Zhang, J.; Milstein, D. Direct Synthesis of Imines from Alcohols and Amines with Liberation of H$_2$. *Angew. Chem. Int. Ed.* **2010,** *49*, 1468-1471.
8. Rezayee, N. M.; Huff, C. A.; Sanford, M. S. Tandem Amine and Ruthenium-Catalyzed Hydrogenation of CO$_2$ to Methanol. *J. Am. Chem. Soc.* **2015,** *137*, 1028-1031.
9. Pell, C. J.; Ozerov, O. V. A series of pincer-ligated rhodium complexes as catalysts for the dimerization of terminal alkynes. *ACS Catal.* **2014,** *4*, 3470-3480.
10. Timpa, S. D.; Pell, C. J.; Ozerov, O. V. A Well-Defined (POCOP)Rh Catalyst for the Coupling of Aryl Halides with Thiols. *J. Am. Chem. Soc.* **2014,** *136*, 14772-14779.
11. Tanaka, R.; Yamashita, M.; Nozaki, K. Catalytic Hydrogenation of Carbon Dioxide Using Ir(III)-Pincer Complexes. *J. Am. Chem. Soc.* **2009,** *131*, 14168-14169.
12. Baratta, W.; Ballico, M.; Chelucci, G.; Siega, K.; Rigo, P. Osmium(II) CNN Pincer Complexes as Efficient Catalysts for Both Asymmetric Transfer and H2 Hydrogenation of Ketones. *Angew. Chem. Int. Ed.* **2008,** *47*, 4362-4365.
13. Gruver, B. C.; Adams, J. J.; Arulsamy, N.; Roddick, D. M. Acceptor Pincer Chemistry of Osmium: Catalytic Alkane Dehydrogenation by (CF$_3$PCP)Os(cod)(H). *Organometallics* **2013,** *32*, 6468-6475.
14. Ohff, M.; Ohff, A.; van der Boom, M. E.; Milstein, D. Highly Active Pd(II) PCP-Type Catalysts for the Heck Reaction. *J. Am. Chem. Soc.* **1997,** *119*, 11687-11688.
15. Morales-Morales, D.; Redón, R.; Yung, C.; Jensen, C. M. High yield olefination of a wide scope of aryl chlorides catalyzed by the phosphinito palladium PCP pincer complex: [PdCl{CH(OPPr)-2,6}]. *Chem. Commun.* **2000**, 1619-1620.
16. Wang, Z.; Feng, X.; Fang, W.; Tu, T. Efficient Aqueous-Phase Heck Reaction Catalyzed by a Robust Hydrophilic Pyridine-Bridged Bisbenzimidazolylidene-Palladium Pincer Complex. *Synlett* **2011,** *2011*, 951-954.
17. Ke, D.; Espinosa, N. A.; Mallet-Ladeira, S.; Monot, J.; Martin-Vaca, B.; Bourissou, D. Efficient Synthesis of Unsaturated δ- and ε-Lactones/Lactams by Catalytic Cycloisomerization: When Pt Outperforms Pd. *Adv. Synth. Catal.* **2016,** *358*, 2324-2331.
18. Valdés, H.; García-Eleno, M. A.; Canseco-Gonzalez, D.; Morales-Morales, D. Recent Advances in Catalysis with Transition-Metal Pincer Compounds. *ChemCatChem* **2018,** *10*, 3136-3172.
19. Ott, J. C.; Blasius, C. K.; Wadepohl, H.; Gade, L. H. Synthesis, Characterization, and Reactivity of a High-Spin Iron(II) Hydrido Complex Supported by a PNP Pincer Ligand and Its Application as a Homogenous Catalyst for the Hydrogenation of Alkenes. *Inorg. Chem.* **2018,** *57*, 3183-3191.

20. Xu, R.; Chakraborty, S.; Bellows, S. M.; Yuan, H.; Cundari, T. R.; Jones, W. D. Iron-Catalyzed Homogeneous Hydrogenation of Alkenes under Mild Conditions by a Stepwise, Bifunctional Mechanism. *ACS Catal.* **2016,** *6*, 2127-2135.

21. Lin, T.-P.; Peters, J. C. Boryl–Metal Bonds Facilitate Cobalt/Nickel-Catalyzed Olefin Hydrogenation. *J. Am. Chem. Soc.* **2014,** *136*, 13672-13683.

22. Vasudevan, K. V.; Scott, B. L.; Hanson, S. K. Alkene Hydrogenation Catalyzed by Nickel Hydride Complexes of an Aliphatic PNP Pincer Ligand. *Eur. J. Inorg. Chem.* **2012,** *2012*, 4898-4906.

23. Rahaman, S. M. W.; Pandey, D. K.; Rivada-Wheelaghan, O.; Dubey, A.; Fayzullin, R. R.; Khusnutdinova, J. R. Hydrogenation of Alkenes Catalyzed by a Non-pincer Mn Complex. *ChemCatChem* **2020,** *12*, 5912-5918.

24. Chirik, P. J. Iron- and Cobalt-Catalyzed Alkene Hydrogenation: Catalysis with Both Redox-Active and Strong Field Ligands. *Acc. Chem. Res.* **2015,** *48*, 1687-1695.

25. Wen, J.; Wang, F.; Zhang, X. Asymmetric hydrogenation catalyzed by first-row transition metal complexes. *Chem. Soc. Rev.* **2021,** *50*, 3211-3237.

26. Weber, S.; Stöger, B.; Veiros, L. F.; Kirchner, K. Rethinking Basic Concepts—Hydrogenation of Alkenes Catalyzed by Bench-Stable Alkyl Mn(I) Complexes. *ACS Catal.* **2019,** *9*, 9715-9720.

27. Gorgas, N.; Brünig, J.; Stöger, B.; Vanicek, S.; Tilset, M.; Veiros, L. F.; Kirchner, K. Efficient Z-Selective Semihydrogenation of Internal Alkynes Catalyzed by Cationic Iron(II) Hydride Complexes. *J. Am. Chem. Soc.* **2019,** *141*, 17452-17458.

28. Alawisi, H.; Arman, H. D.; Tonzetich, Z. J. Catalytic Hydrogenation of Alkenes and Alkynes by a Cobalt Pincer Complex: Evidence of Roles for Both Co(I) and Co(II). *Organometallics* **2021,** *40*, 1062-1070.

29. Junge, K.; Papa, V.; Beller, M. Cobalt–Pincer Complexes in Catalysis. *Chem. Eur. J.* **2019,** *25*, 122-143.

30. Rummelt, S. M.; Zhong, H.; Léonard, N. G.; Semproni, S. P.; Chirik, P. J. Oxidative Addition of Dihydrogen, Boron Compounds, and Aryl Halides to a Cobalt(I) Cation Supported by a Strong-Field Pincer Ligand. *Organometallics* **2019,** *38*, 1081-1090.

31. Pabst, T. P.; Obligacion, J. V.; Rochette, É.; Pappas, I.; Chirik, P. J. Cobalt-Catalyzed Borylation of Fluorinated Arenes: Thermodynamic Control of C(sp^2)-H Oxidative Addition Results in ortho-to-Fluorine Selectivity. *J. Am. Chem. Soc.* **2019,** *141*, 15378-15389.

32. Scheuermann, M. L.; Semproni, S. P.; Pappas, I.; Chirik, P. J. Carbon Dioxide Hydrosilylation Promoted by Cobalt Pincer Complexes. *Inorg. Chem.* **2014,** *53*, 9463-9465.

33. Semproni, S. P.; Hojilla Atienza, C. C.; Chirik, P. J. Oxidative addition and C-H activation chemistry with a PNP pincer-ligated cobalt complex. *Chem. Sci.* **2014,** *5*, 1956-1960.

34. Khaskin, E.; Diskin-Posner, Y.; Weiner, L.; Leitus, G.; Milstein, D. Formal loss of an H radical by a cobalt complex via metal-ligand cooperation. *Chem. Commun.* **2013,** *49*, 2771-2773.

35. Park, Y.; Semproni, S. P.; Zhong, H.; Chirik, P. J. Synthesis, Electronic Structure, and Reactivity of a Planar Four-Coordinate, Cobalt–Imido Complex. *Angew. Chem. Int. Ed. 60*, 14376-14380.

36. Neely, J. M.; Bezdek, M. J.; Chirik, P. J. Insight into Transmetalation Enables Cobalt-Catalyzed Suzuki–Miyaura Cross Coupling. *ACS Cent. Sci.* **2016,** *2*, 935-942.

37. Obligacion, J. V.; Semproni, S. P.; Pappas, I.; Chirik, P. J. Cobalt-Catalyzed C(sp^2)-H Borylation: Mechanistic Insights Inspire Catalyst Design. *J. Am. Chem. Soc.* **2016,** *138*, 10645-10653.

38. Obligacion, J. V.; Bezdek, M. J.; Chirik, P. J. C(sp^2)-H Borylation of fluorinated arenes using an air-stable cobalt precatalyst: electronically enhanced site selectivity enables synthetic opportunities. *J. Am. Chem. Soc.* **2017,** *139*, 2825-2832.

39. Arevalo, R.; Chirik, P. J. Enabling Two-Electron Pathways with Iron and Cobalt: From Ligand Design to Catalytic Applications. *J. Am. Chem. Soc.* **2019,** *141*, 9106-9123.

40. Sun, J.; Luo, L.; Luo, Y.; Deng, L. An NHC−Silyl−NHC Pincer Ligand for the Oxidative Addition of C−H, N−H, and O−H Bonds to Cobalt(I) Complexes. *Angew. Chem. Int. Ed.* **2017,** *56*, 2720-2724.

41. Lapointe, S.; Khaskin, E.; Fayzullin, R. R.; Khusnutdinova, J. R. Stable Nickel(I) Complexes with Electron-Rich, Sterically-Hindered, Innocent PNP Pincer Ligands. *Organometallics* **2019,** *38*, 1581-1594.

42. Lapointe, S.; Khaskin, E.; Fayzullin, R. R.; Khusnutdinova, J. R. Nickel(II) Complexes with Electron-Rich, Sterically Hindered PNP Pincer Ligands Enable Uncommon Modes of Ligand Dearomatization. *Organometallics* **2019,** *38*, 4433-4447.

43. Khaskin, E.; Fayzullin, R. R.; Deolka, S. Bulky PNP Ligands Blocking Metal-Ligand Cooperation Allow for Isolation of Ru(0), and Lead to Catalytically Active Ru Complexes in Acceptorless Alcohol Dehydrogenation. *ChemRxiv*, 10.26434/chemrxiv.14612262.v1.

44. Addison, A. W.; Rao, T. N.; Reedijk, J.; van Rijn, J.; Verschoor, G. C. Synthesis, structure, and spectroscopic properties of copper(II) compounds containing nitrogen ‐ sulphur donor ligands; the crystal and molecular structure of aqua[1,7-bis(N-methylbenzimidazol-2 ′ -yl)-2,6-dithiaheptane]copper(II) perchlorate. *J. Chem. Soc., Dalton Trans.* **1984**, 1349-1356.

45. Khusnutdinova, J. R.; Luo, J.; Rath, N. P.; Mirica, L. M. Late First-Row Transition Metal Complexes of a Tetradentate Pyridinophane Ligand: Electronic Properties and Reactivity Implications. *Inorg. Chem.* **2013,** *52*, 3920-3932.

46. Shaffer, D. W.; Bhowmick, I.; Rheingold, A. L.; Tsay, C.; Livesay, B. N.; Shores, M. P.; Yang, J. Y. Spin-state diversity in a series of Co(II) PNP pincer bromide complexes. *Dalton Trans.* **2016,** *45*, 17910-17917.

47. Krivokapic, I.; Zerara, M.; Daku, M. L.; Vargas, A.; Enachescu, C.; Ambrus, C.; Tregenna-Piggott, P.; Amstutz, N.; Krausz, E.; Hauser, A. Spin-crossover in cobalt(II) imine complexes. *Coord. Chem. Rev.* **2007,** *251*, 364-378.

48. Okuniewski, A.; Rosiak, D.; Chojnacki, J.; Becker, B. Coordination polymers and molecular structures among complexes of mercury(II) halides with selected 1-benzoylthioureas. *Polyhedron* **2015,** *90*, 47-57.

49. Rosiak, D.; Okuniewski, A.; Chojnacki, J. Novel complexes possessing Hg–(Cl, Br, I)···OC halogen bonding and unusual $Hg_2S_2(Br/I)_4$ kernel. The usefulness of τ_4' structural parameter. *Polyhedron* **2018,** *146*, 35-41.

50. Crabtree, R. H. Dihydrogen complexes: some structural and chemical studies. *Acc. Chem. Res.* **1990,** *23*, 95-101.

51. Heinekey, D. M.; Oldham, W. J. Coordination chemistry of dihydrogen. *Chem. Rev.* **1993,** *93*, 913-926.

52. Desrosiers, P. J.; Cai, L.; Lin, Z.; Richards, R.; Halpern, J. Assessment of the "T_1 criterion" for distinguishing between classical and nonclassical transition-metal hydrides: hydride relaxation rates in tris(triarylphosphine)osmium tetrahydrides and related polyhydrides. *J. Am. Chem. Soc.* **1991,** *113*, 4173-4184.

53. Heinekey, D. M.; van Roon, M. Dihydride Complexes of the Cobalt and Iron Group Metals: An Investigation of Structure and Dynamic Behavior. *J. Am. Chem. Soc.* **1996,** *118*, 12134-12140.

54. Morris, R. H. Dihydrogen, dihydride and in between: NMR and structural properties of iron group complexes. *Coord. Chem. Rev.* **2008,** *252*, 2381-2394.

55. Rozenel, S. S.; Padilla, R.; Camp, C.; Arnold, J. Unusual activation of H_2 by reduced cobalt complexes supported by a PNP pincer ligand. *Chem. Commun.* **2014,** *50*, 2612-2614.

56. De Buysser, K.; Herman, G. G.; Bruneel, E.; Hoste, S.; Van Driessche, I. Determination of the number of unpaired electrons in metal-complexes. A comparison between the Evans' method and susceptometer results. *Chem. Phys.* **2005,** *315*, 286-292.

57. Bain, G. A.; Berry, J. F. Diamagnetic Corrections and Pascal's Constants. *J. Chem. Educ.* **2008,** *85*, 532.